

Interbank Asset-Liability Networks with Fire Sale Management

by Zachary Feinstein¹ and Grzegorz Halaj²

¹Stevens Institute of Technology

²Financial Stability Department
Bank of Canada, Ottawa, Ontario, Canada K1A 0G9

gahalaj@bankofcanada.ca, zfeinste@stevens.edu

Bank of Canada staff working papers provide a forum for staff to publish work-in-progress research independently from the Bank's Governing Council. This research may support or challenge prevailing policy orthodoxy. Therefore, the views expressed in this paper are solely those of the authors and may differ from official Bank of Canada views. No responsibility for them should be attributed to the Bank.



Acknowledgements

We would like to thank an anonymous referee, Ruben Hipp, the Banff International Research Centre, Tom Hurd, and participants of the Analytical Methods for Financial Systemic Risk workshop (Banff), as well as participants of a research seminar of the Bank of Canada, for their comments. We would also like to thank Nicolas Whitman for excellent research assistance.

Abstract

Interconnectedness is an inherent feature of the modern financial system. While it contributes to efficiency of financial services, it also creates structural vulnerabilities: pernicious shock transmission and amplification impacting banks' capitalization. This has recently been seen during the Global Financial Crisis. Post-crisis reforms addressed many of the causes of the problems. But contagion effects may not be fully eliminated. One reason for this may be related to financial institutions' incentives and strategic behaviours. We propose a model to study contagion effects in a banking system, capturing network effects of direct exposures and indirect effects of market behaviour that may impact asset valuation. By doing so, we can embed a well-established fire sale channel into our model. Unlike in related literature, we relax an assumption of an exogenous pecking order of how banks would sell their assets. Instead, banks act rationally in our model; they optimally construct a portfolio subject to budget constraints to raise cash to satisfy creditors (interbank and external). We assume that the guiding principle for banks is to maximize risk-adjusted returns generated by their balance sheets. We parameterize the theoretical model with confidential supervisory data for banks in Canada under the supervision of the Office of the Superintendent of Financial Institutions, which allows us to run simulations of bank valuations and asset prices under a set of stress scenarios.

Bank topics: Financial stability; Financial system regulation and policies; Payment clearing and settlement systems

JEL codes: C, C6, C62, C63, C7, C72, G, G01, G1, G11

1 Introduction

Interconnectedness is an inherent feature of the modern financial system. These interconnections, in normal times, increase the efficiency of the banking system and financial services. This includes the ability for individuals and institutions to invest more appropriately to manage risk and hit target returns. In the best case, these interconnections in the financial system can even mitigate losses from idiosyncratic shocks because of increased diversification of investment opportunities. However, as witnessed in the Global Financial Crisis, the interconnections between financial institutions also create structural vulnerabilities that allow for contagion and amplification of systematic shocks. In this work we focus on two primary modes of financial contagion: interbank obligations and portfolio overlap. These modes of contagion are often referred to as *default contagion* and *price-mediated contagion* respectively.

Due to the Global Financial Crisis, reforms and new regulations have been implemented to address many of the causes of that specific crisis (FSB, 2016). These reforms include new regulations for “too big to fail” financial institutions and the encouragement of central clearing parties to reduce counterparty risks in many over-the-counter markets. Though these reforms are targeted at the precipitating causes of the Global Financial Crisis, financial contagion remains a threat to the health of the financial system. Financial contagion may be less related to direct interconnectedness via lending and borrowing between financial institutions and more to indirect links via similarities of their balance sheets and financial complexity. For instance, based on information collected by the Basel Committee on Banking Supervision to determine global systemically important banks (G-SIBs) we can see that even though interconnectedness dropped slightly in recent years, complexity did less so (see Figure 1). Moreover, international authorities such as the Financial Stability Board (see FSB (2020)) and the Bank of International Settlements emphasize that¹ “[...]despite progress made by macro prudential policy, we have been less good at making the global financial system more resilient as an interconnected system.”

Default contagion and price-mediated contagion are financial concepts that are well-established in the mathematical finance literature. Default contagion occurs as a result of the direct exposures between financial institutions. We take the model of Eisenberg and Noe (2001) as the foundation for studying default contagion. Banks are connected through a network of obligations; the default of one bank causes losses in the balance sheet of its counterparties and thus can trigger a cascade of further defaults. Though not utilized in this work, the framework of Eisenberg and Noe (2001) has been extended to include, e.g., bankruptcy costs (Rogers and Veraart, 2013), equity cross-holdings (Suzuki, 2002; Gouriéroux et al., 2012), and contingent claims such as credit default swaps (Schuldenzucker et al., 2019; Klages-Mundt and Minca, 2020; Banerjee

¹Remarks of Benoit Coeure “Learning the value of resilience and technology: the global financial system after Covid-19”, <https://www.bis.org/speeches/sp200417.htm>.

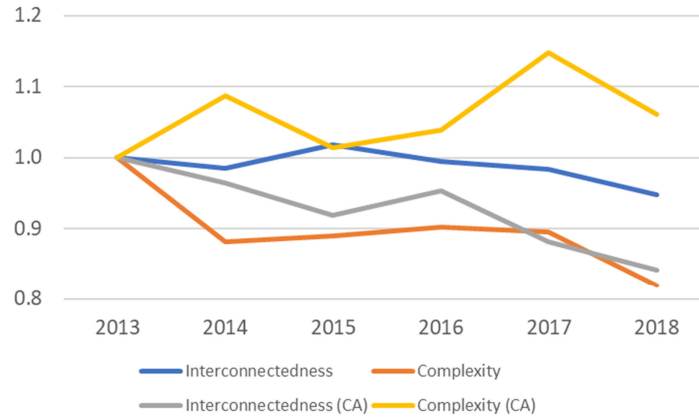


Figure 1: Indicators of interconnectedness and complexity used to determine G-SIB classification of banks. Dynamics normalized with 2013 at 1.0. Data from https://www.bis.org/bcbs/gsib/hl_ind_since_2013.xlsx.

“Interconnectedness” – intra-financial assets and liabilities and securities outstanding;

“Complexity” – trading and available for sale securities indicator;

(CA) – indicators calculated only for five Canadian banks.

and Feinstein, 2019). Price-mediated contagion occurs due to the indirect interactions between financial institutions via the price of commonly held assets; prices drop when a bank sells assets, and, following mark-to-market valuation, the balance sheets of all firms are impacted. This phenomenon is closely related to the fire sales when prices of assets in forced transactions deviate from their fundamental values. It was thoroughly described by Shleifer and Vishny (2011). These portfolio overlaps, which to a large extent are a consequence of risk regulation that promotes diversification of assets, can be a serious channel for contagion. We wish to highlight the work of Weber and Weske (2017), which summarizes multiple of these contagion models in a single work.

Many papers on price-mediated contagion and fire sales begin with the Eisenberg and Noe (2001) framework for interbank obligations. Within this framework, Cifuentes et al. (2005); Amini et al. (2016); Braverman and Minca (2018) and Calimani et al. (2019) study the existence and uniqueness of joint clearing payments and prices in systems with both interbank liabilities and a single marketable illiquid asset subject to fire sale dynamics. This notion is extended to include multiple illiquid assets in numerous works. The most common liquidation strategy undertaken is mechanistic and assumes proportional selling of all assets (Greenwood et al., 2015; Duarte and Eisenbach, 2018; Cont and Schaanning, 2019; Feinstein, 2020). However, recent literature has considered banks to be utility maximizers (Feinstein, 2017, 2019; Braouezec and

Wagalath, 2019; Banerjee and Feinstein, 2020). Equilibrium interbank payments and prices of assets used to supplement liquidity after a shock were studied by Caballero and Simsek (2013) but with an assumption of an imperfectly observed structure of the market.

Our methodological contribution to the literature is about capturing strategic management actions of banks in a networked financial market. In this work, banks are assumed to be utility maximizers who may choose to fully rebalance their portfolios. To the best of our knowledge, such a specification of banks' objectives to maximize utility from the rebalancing of the entire portfolio to raise cash and satisfy interbank and external creditors is a novelty in the literature. In coming to their optimal decisions, banks consider fluctuations in prices, the defaults of counterparties in a network of financial exposures, or even the market transactions of other banks. This modelling framework follows the structure of Feinstein (2019) to consider both default and price-mediated contagion. In this setup, we are able to demonstrate the existence of banks' strategies in equilibrium that combine interbank payments, asset holdings, and asset prices. Notably, by straightforward modification of portfolio constraints, the model can be set up to study the price impact of either reinvestment decisions (i.e., rebalancing of assets) or optimal liquidation strategies (i.e., selling of assets).

To test our theoretical model, we calibrate it with confidential supervisory data for the largest Canadian banks under the supervision of the Office of the Superintendent of Financial Institutions. We run stress-test scenarios on this dataset. Notably, rather than focusing solely on clearing equilibria, the modelling and simulations consider the procedure in which markets reach clearing through the tâtonnement process. As highlighted later in this work, if an equilibrium is not reached, such a procedure endogenously generates market dynamics that look akin to noise. We also show how flexible our framework is to incorporate a market regulator whose objective is to stabilize liquidity in the distressed financial system.

This paper is organized as follows. In Section 2, we present the theoretical model utilized in this work. In order to do that we present the stylized balance sheet and rules for interactions between banks. Existence of equilibria is proven and the tâtonnement process is proposed. In Section 3, we present a utility function utilized in our case studies that encodes the risk-adjusted returns taking other banks' actions into account. We additionally provide a method for calibrating this utility function to data. In Section 4, we calibrate this theoretical model to the confidential supervisory data of Canadian banks and undertake stress tests of this banking system in our framework; Section 5 concludes.

2 Market clearing and the tâtonnement process

Consider a system of N banks indexed by $i \in \{1, \dots, N\}$. Each bank is interconnected in two ways: through interbank obligations and through portfolio overlaps. More explicitly, the balance sheet of bank i is made up of assets:

- cash account ($a_i \geq 0$);
- M marketable external assets ($x_{im} \geq 0$ for asset $m \in \{1, \dots, M\}$);
- a pool of illiquid, non-marketable assets ($\tilde{x}_i \geq 0$); and
- interbank assets ($\sum_{j=1}^N L_{ji}$ for nominal obligations $L_{ji} \geq 0$ from bank j)

and liabilities:

- interbank funding, i.e., the sum of deposits from all other banks ($\bar{p}_i := \sum_{j=1}^N L_{ij}$);
- external funding ($z_i \geq 0$); and
- capital (c_i).

A fraction $\delta_i \in [0, 1]$ of the external funding sources is subject to funding risk. This assumption reflects rollover risk (i.e., the risk that maturing funding is not renewed or it is impossible to replace it) or the risk of runs (i.e., if funding providers call the debt that they granted). This parameter δ will be used in simulations of funding shocks in case studies presented in Section 4. For notational simplicity, we will denote the total funding on bank i 's balance sheet that has to be satisfied as $\bar{P}_i := \bar{p}_i + \delta_i z_i$. Following, e.g., (Eisenberg and Noe, 2001), we assume that no bank accumulates any positive equity until all debts are paid in full and, consequently, the balance sheet identity holds for any bank i

$$c_i = a_i + \tilde{x}_i + \sum_{m=1}^M x_{im} + \sum_{j=1}^N L_{ji} - (1 - \delta_i)z_i - \bar{P}_i.$$

Assumption 2.1. *As validated in the data, we will assume throughout this work that all banks i have positive external assets $a_i + \sum_{m=1}^M x_{im} > 0$ and liabilities $\bar{P}_i > 0$.*

The clearing model under consideration is constructed from two interrelated contagion mechanisms: interbank payments and price impacts.

- For the interbank payments, we follow limited liabilities in that no bank will pay more than its total available assets. Following the rule set from Eisenberg and Noe (2001), we additionally assume

throughout this work that all obligations have the same seniority. We consider the relative exposures of bank i to bank j by $\pi_{ji} := L_{ji}/\bar{P}_j$. As such, the inflows to bank i from interbank payments are given by $\sum_{j=1}^N \pi_{ji} p_j$, where $p_j \in [0, \bar{P}_j]$ is the payments made by bank j , which is determined in an equilibrium (clearing) procedure detailed below in (1).

- For the price impacts on marketable external assets, we introduce the collection of inverse demand functions $f_m : \mathbb{R} \rightarrow [\underline{q}_m, \bar{q}_m] \subseteq \mathbb{R}_{++}$ for each asset type $m \in \{1, \dots, M\}$. Each inverse demand function provides a price generated by the market based on the aggregate liquidations in that asset. As undertaken in Feinstein (2019), these inverse demand functions can accept positive inputs (the asset is, on net, being sold by the banks) or negative inputs (the asset is, on net, being bought by the banks); this is in contrast to earlier works on price-mediated contagion, e.g., (Greenwood et al., 2015; Amini et al., 2016; Feinstein, 2017), in which banks are constrained so as to only liquidate assets. Without loss of generality, consider $f_m(0) = 1$ for every asset type m so that x_{im} denotes both the physical units of asset m held by bank i and the (pre-fire sale) value of those assets. Additionally, these inverse demand functions are assumed to be continuous and non-increasing in net asset liquidations. As such, the cash extracted from the marketable external assets (if positive) by bank i is provided by $\sum_{m=1}^M f_m(\sum_{j=1}^N v_{jm}) v_{im}$, where v_{jm} is the volume of assets of type m that are liquidated by bank j . Note that the impact of transacted volumes on prices may induce banks to alter their trading strategies in the equilibrium (clearing) procedure.

Assumption 2.2. *For the remainder of this work, we will assume that each inverse demand function has the linear structure $f_m(v) := 1 - b_m v$ for $b_m \in (0, \frac{1}{2 \sum_{i=1}^N x_{im}})$. With this construction, the lower bound on the price of asset m is thus given by*

$$\underline{q}_m := 1 - b_m \sum_{i=1}^N x_{im} \in \left(\frac{1}{2}, 1\right)$$

and the upper bound is given by

$$\bar{q}_m := \frac{1 + \sqrt{1 + 4b_m \sum_{i=1}^N \left(a_i + \sum_{\tilde{m} \neq m} x_{i\tilde{m}} \underline{q}_{\tilde{m}} + \sum_{j=1}^N L_{ji} - \bar{P}_i \right)^+}}{2} \geq 1.$$

The clearing payments are determined in an Eisenberg-Noe framework when the prices of all marketable assets $q \in [\underline{q}_1, \bar{q}_1] \times \dots \times [\underline{q}_M, \bar{q}_M]$ are fixed. That is, define the payment clearing mapping $\Psi : [0, \bar{P}_1] \times \dots \times$

$[0, \bar{P}_n] \times [\underline{q}_1, \bar{q}_1] \times \cdots \times [\underline{q}_M, \bar{q}_M] \rightarrow [0, \bar{P}_1] \times \cdots \times [0, \bar{P}_n]$ for bank i as

$$\Psi_i(p, q) = \left(a_i + \sum_{m=1}^M q_m x_{im} + \sum_{j=1}^N \pi_{ji} p_j \right) \wedge \bar{P}_i. \quad (1)$$

The clearing payment vector p^* under current market prices q is found as the fixed point of Ψ . Denote $p^*(q) = \Psi(p^*(q), q)$ to be the Eisenberg-Noe clearing payment vector under market prices $q \in [\underline{q}_1, \bar{q}_1] \times \cdots \times [\underline{q}_m, \bar{q}_m]$; $p^*(q)$ is unique due to Assumption 2.1 and (Eisenberg and Noe, 2001, Theorem 2).

In much the same way as considered by Feinstein (2019), banks are free to rebalance their cash account and marketable assets but constrained so as to satisfy their obligations. We further impose a no-short-selling constraint. Rather than working directly on asset liquidations and purchases, consider the asset holdings $y_{im} \geq 0$ (for bank i and asset type m). The net amount of asset m liquidated by the banks is thus provided by $v_m = \sum_{j=1}^N [x_{jm} - y_{jm}]$. Furthermore, by buying and selling these marketable assets, each bank's cash account updates as well; given market prices q and clearing payments $p^*(q)$, this cash account for bank i would be given by

$$a_i^* := a_i + \sum_{m=1}^M q_m [x_{im} - y_{im}] + \sum_{j=1}^N \pi_{ji} p_j^*(q).$$

With the notion that banks do not accumulate equity until all debts are paid in full, it must follow that

$$a_i^* \geq \left(a_i + \sum_{m=1}^M q_m x_{im} + \sum_{j=1}^N \pi_{ji} p_j^*(q) \right) \wedge \bar{P}_i.$$

Therefore, in order to satisfy its obligations, bank i must invest so as to have enough cash to cover its payments, i.e.,

$$\sum_{m=1}^M q_m y_{im} \leq \left[a_i + \sum_{m=1}^M q_m x_{im} + \sum_{j=1}^N \pi_{ji} p_j^*(q) - \bar{P}_i \right]^+. \quad (2)$$

This constraint can be viewed as a budget constraint since it provides an upper bound on the investments made. The constraint is related to the capital value available to each bank given payments $p^*(q)$ and market prices q . Note that banks are allowed to hold excess cash at the end of the clearing procedure because of the inequality-based budget constraint.

Remark 2.3. The traditional fire sale literature, e.g., (Greenwood et al., 2015; Amini et al., 2016; Feinstein, 2017), constrains banks to only liquidate marketable assets, and to generate no excess cash reserves from doing so, during the clearing procedure. Such constraints can be included in the clearing procedure by including the additional rule that $y_{im} \leq x_{im}$ and forcing equality in the budget constraint (2). No other alterations would be required for that setting.

It remains to show how each bank will trade in order to determine their optimal portfolio given clearing payments $p^*(q)$ and market prices q . We assume that each bank is a portfolio optimizer following some strictly concave utility function. That is, bank i seeks to maximize the utility $u_i(y_i, y_{-i}^*)$. Consequently, bank i is a portfolio optimizer solving

$$y_i^\dagger(y^*, q) = \arg \max \{u_i(y_i, y_{-i}^*) \mid y_i \in \mathcal{A}_i(q)\}$$

$$\mathcal{A}_i(q) = \left\{ y_i \in \mathbb{R}_+^M \mid \sum_{m=1}^M q_m y_{im} \leq \left[a_i + \sum_{m=1}^M q_m x_{im} + \sum_{j=1}^N \pi_{ji} p_j^*(q) - \bar{P}_i \right]^+ \right\}.$$

Notably, by the construction of y^\dagger , if a bank is defaulting (i.e., assets have less value than the total obligations), then it will hold no marketable assets because of the no-short-selling and budgetary constraints.

Assumption 2.4. *The utility function u_i is strictly concave for every bank i . As a consequence, $y_i^\dagger(y^*, q)$ is a singleton for any portfolio holdings y^* and market prices q .*

The full clearing procedure is joint in market prices q^* and portfolio holdings y^* described by

$$q^* = f \left(\sum_{i=1}^N [x_i - y_i^*] \right), \quad y^* = y^\dagger(y^*, q^*). \quad (3)$$

The clearing cash account for bank i would, as discussed above, be determined by

$$a_i^* = a_i + \sum_{m=1}^M q_m^* [x_{im} - y_{im}^*] + \sum_{j=1}^N \pi_{ji} p_j^*(q^*).$$

Excess cash reserves, after clearing, can then be computed simply as $(a_i^* - \bar{P}_i)^+$.

By construction of y^\dagger , any clearing portfolio holdings (and therefore also the cash account) is a Nash equilibrium. That is, fixing the strategy of all other banks y_{-i}^* and the prices q^* , bank i cannot obtain a higher utility than $u_i(y^*)$.

Proposition 2.5. *There exists a clearing solution q^*, y^* to (3).*

Proof. First, by Lemma 5 of Eisenberg and Noe (2001), p^* is continuous as a function of the market prices q ; and, by the Berge maximum theorem, y^\dagger is jointly continuous in (y^*, q^*) . Thus, existence trivially follows for $q^* = f \left(\sum_{i=1}^N [x_i - y_i^*] \right)$ and $y^* = y^\dagger(y^*, q^*)$ by the Brouwer fixed point theorem. \square

Rather than concerning ourselves, explicitly, with considering an equilibrium solution, as in Feinstein (2019), we consider a specific tâtonnement process; the one we consider herein is on the space of portfolio

holdings rather than prices as undertaken in Feinstein (2019). Namely, consider the tâtonnement process:

$$dy_t = \text{sign} \left(y^\dagger(y_t, f \left(\sum_{i=1}^N [x_i - y_{i,t}] \right)) - y_t \right) \otimes \Delta_y dt, \quad y_0 = x, \quad (4)$$

where Δ_y denotes the velocity of market orders and \otimes denotes the Hadamard product. The resulting market prices over time can be computed explicitly by

$$q_t = f \left(\sum_{i=1}^N [x_i - y_{i,t}] \right)$$

and $q_0 = \vec{1}$ by construction.

Algorithm 2.6. The tâtonnement process can be simulated via an application of Euler's method as the following:

1. Initialize $t = 0$, $\Delta t > 0$, $\epsilon > 0$, $\Delta_y := \epsilon x$, $q_t = \vec{1}$, and $y_t = x$;
2. While $t \leq T$ for some sufficiently large time T :
 - (a) Initialize $k = 0$, $p^{(0)} = \bar{P}$, and $\mathcal{D}^{(0)} = \emptyset$;
 - (b) Iterate $k = k + 1$;
 - (c) Define $\mathcal{D}^{(k)} = \{i \mid a_i + \sum_m q_{t,m} x_{im} + \sum_j \pi_{ji} p_j^{(k-1)} < \bar{P}_j\}$;
 - (d) If $\mathcal{D}^{(k)} = \mathcal{D}^{(k-1)}$ then go to step (2h) with $p^* = p^{(k-1)}$;
 - (e) Set $\Lambda \in \{0, 1\}^{N \times N}$ such that $\Lambda_{ii} = 1$ if $i \in \mathcal{D}^{(k)}$ and 0 otherwise;
 - (f) Update $p^{(k)} = (I - \Lambda \Pi^\top)^{-1} [(I - \Lambda) \bar{P} + \Lambda (a + \sum_m q_{t,m} x_{.m})]$;
 - (g) Return to step (2b);
 - (h) For each bank i , define the feasible region \mathcal{A}_i as

$$\mathcal{A}_i = \left\{ y_i \in \mathbb{R}_+^M \mid \sum_{m=1}^M q_{m,t} y_{im} \leq \left[a_i + \sum_{m=1}^M q_{m,t} x_{im} + \sum_{j=1}^N \pi_{ji} p_j^* - \bar{P}_i \right]^+ \right\};$$

- (i) For each bank i , define y_i^\dagger as

$$y_i^\dagger = \arg \max \{ u_i(y_i, y_{-i,t}) \mid y_i \in \mathcal{A}_i \};$$

- (j) Update $y_{t+\Delta t} = y_t + \text{sign}([y^\dagger - y_t]) \otimes \Delta_y$ and $q_{t+\Delta t} = f \left(\sum_{i=1}^N [x_i - y_{i,t+\Delta}] \right)$;

(k) Increment $t = t + \Delta t$.

There are two possible conclusions from the tâtonnement process (4). If the tâtonnement process limits to a single point, then this is an equilibrium (clearing) vector of market holdings y^* with associated prices q^* ; see Proposition 2.7. The associated payment vector can be found as $p^*(q^*)$. However, if the tâtonnement process does not converge, then (as the portfolio holdings take value in a compact box as shown in the proof of Corollary 3.11 of Feinstein (2019)) the portfolio holdings and, therefore, prices fluctuate in a, perhaps irregular, cycle. In such a situation, we naturally recover a notion of “noise” in the price of the marketable assets; without additional modifications of system parameters, the prices of the different asset types will fluctuate in relation to each other. As the time in the tâtonnement process is fictitious, these fluctuations can occur rapidly and appear as noise in the pricing process. Notably, this observed noise would be endogenous to the system without the need for any exogenous stochastic processes. Though Proposition 2.5 provides existence criteria for an equilibrium solution, this tâtonnement process can be utilized even if that concavity criteria is not satisfied (though there may be challenges with computing y^\dagger for the non-concave maximization problems).

Proposition 2.7. *If the tâtonnement process (4) converges to a point y^* , then $q^* := f(\sum_{i=1}^N [x_i - y_i^*])$ and y^* define a clearing solution of (3).*

Proof. y^* is a point of convergence of (4) if and only if $y^\dagger(y^*, q^*) = y^*$ for $q^* = f(\sum_{i=1}^N [x_i - y_i^*])$. Recall the definition of a clearing solution from (3) and the proof is complete. \square

3 Risk-adjusted return utility

In this section we propose a class of financially meaningful utility functions for consideration in Section 4. We wish to note that the tâtonnement process proposed above in (4) can be utilized with other utility functions (including heterogeneous utilities for different institutions). Broadly, this utility function corresponds to banks being risk-adjusted return optimizers.

More specifically, consider the setting in which bank i seeks to maximize risk-adjusted returns where returns are measured with respect to the inverse demand function f . That is, the return of a portfolio y_i is the aggregate of the returns $\mu^\top y_i$, losses on the liquidated volume $x - y$, and losses due to the revaluation of the holdings with a rebound factor $\beta_i \in [0, 1]^M$. Furthermore, bank i will adjust its returns through the covariance structure C with risk aversion $\gamma_i \geq 0$. Mathematically, this is all combined into the single utility

function

$$u_i(y) = y_i^\top \left(\mu - (I - \text{diag}(\beta_i))[\vec{1} - f(\sum_{j=1}^N [x_j - y_j])] \right) - (x_i - y_i)^\top \left(\vec{1} - f(\sum_{j=1}^N [x_j - y_j]) \right) - \frac{\gamma_i}{2} y_i^\top C y_i.$$

Thus, bank i 's objective is to design asset liquidations (or purchases) to maximize the risk-adjusted return on the outstanding (post-fire sale) assets. To summarize, this objective comprises:

1. *Expected returns*: $\mu^\top y_i$;
2. *Liquidation costs* on volume $x_i - y_i$: $-(x_i - y_i)^\top \left(\vec{1} - f(\sum_{j=1}^N [x_j - y_j]) \right)$;
3. *Revaluation losses* of holdings y_i with mark-to-market elasticity β_i : $-y_i^\top (I - \text{diag}(\beta_i)) [\vec{1} - f(\sum_{j=1}^N [x_j - y_j])]$, where $\text{diag}(\beta_i)$ is a diagonal matrix with entries of β_i on the diagonal;
4. *Risk-adjustment*: $-\frac{\gamma_i}{2} y_i^\top C y_i$.

Recall from Assumption 2.2 that (for simplicity) the inverse demand function $f_m(v) = 1 - b_m v$ has a linear structure with $b_m \in (0, \frac{1}{2 \sum_{i=1}^N x_{im}})$. Thus, the utility function can be simplified to the quadratic structure:

$$u_i(y) = - \left[y_i^\top \left(\text{diag}(\beta_i) \text{diag}(b) + \frac{\gamma_i}{2} C \right) y_i - \left(\mu + \text{diag}(b) \left[x_i + \text{diag}(\beta_i) \left(\sum_{j=1}^N x_j - \sum_{j \neq i} y_j \right) \right] \right)^\top y_i \right]$$

with difference only up to a constant with respect to y_i . Thus, this objective is strictly concave so long as $\text{diag}(\beta_i) \text{diag}(b) + \frac{\gamma_i}{2} C$ is positive definite; this is guaranteed so long as $\beta_i, b \in \mathbb{R}_{++}^M$.

We wish to conclude this section with consideration of the calibration of the bank-specific parameters, i.e., the rebound factor $\beta_i \in [0, 1]^M$ and the risk-aversion $\gamma_i \geq 0$. This calibration is done so that each bank i , when unconstrained, would (approximately) seek to invest in portfolio x_i . Though we present this calibration for the *quantities* invested, x_i is also the vector of (pre-fire sale) values invested in each asset by bank i . This is due to the normalization of the inverse demand function so that $f_m(0) = 1$ for each asset m . Therefore, the calibration presented can, equally, be viewed as a procedure on the *value* invested in each asset rather than the quantity.

In order to construct a tractable calibration, consider the first-order conditions for maximizing the utility u_i for bank i given that all other banks hold their initial portfolios x_{-i} , i.e., the optimal investment y_i^* satisfies

$$\nabla_{y_i} u_i(y_i^*, x_{-i}) = -2 \left(\text{diag}(b) \text{diag}(\beta_i) + \frac{\gamma_i}{2} C \right) y_i^* + (\mu + \text{diag}(b)[I + \text{diag}(\beta_i)]x_i) = \vec{0}.$$

As we are seeking β_i, γ_i so that $y_i^* \approx x_i$, we consider the linear mapping

$$g_i(\beta_i, \gamma_i) := \text{diag}(x_i) \text{diag}(b)\beta_i + [Cx_i]\gamma_i - \mu - \text{diag}(b)x_i$$

which is equal to $\nabla_{y_i} u_i(x_i, x_{-i})$ at β_i, γ_i . We can, therefore, calibrate the system by finding the bank-specific rebound factor β_i and risk-aversion γ_i as the minimizers of the quadratic program

$$\min \{ \|g_i(\beta_i, \gamma_i)\|_2^2 \mid \beta_i \in [0, 1]^M, \gamma_i \geq 0 \}. \quad (5)$$

This calibration procedure is undertaken for all banks in the system to produce the heterogeneous utility functions u_i .

4 Case studies

In this section we consider an in-depth case study and stress test of the Canadian banking system. First, in Section 4.1, we present the dataset and model calibration. This data is then used in Section 4.2 to complete numerical stress tests of the Canadian banking system.

4.1 Canadian banking system data

We apply the model to the Canadian banking system. We focus on a representative subset of Canadian banks. In particular, we consider six domestic systemically important bank (D-SIB) that account for about 90% of the total assets in the Canadian banking system. To this end, we utilize the confidential supervisory data collected by the Canadian supervisory authority, the Office of the Superintendent of Financial Institutions (OSFI). The data are received from D-SIBs in the so-called financial returns. We collected a time series of quarterly data between 2015-06-30 and 2018-12-31 (i.e., 14 snapshots ranging from the second quarter of 2015 through the fourth quarter of 2018). We use three types of the returns: EB/ET, NCCF and BCAR. The EB/ET contains information about interbank exposures and allows us to build an interbank network. We combine three types of instruments to construct the network: direct bank lending, debt instruments issued by the D-SIBs and cross-held by them, and derivatives exposures. We do not differentiate between instruments and aggregate the three types of exposures. Consequently, we obtain one interbank network for a given snapshot of data. The network structure is illustrated in Figure 3. It is a fully connected network, although there is some degree of heterogeneity in terms of the sizes of exposures. The NCCF return breaks down banks' balance sheets into liquidity buckets (see Table 1). Only part of a bank's assets can be used as

a liquidity buffer, i.e., liquidated to generate cash to satisfy immediate obligations. The illiquid fraction of the balance sheet can be quite substantial (on average almost 40% of the D-SIBs’ balance sheets). The liquid or less liquid assets are grouped in a potential liquidity buffer presented in the Table 1. The composition of liquid and less liquid assets remained rather stable in time as shown in Figure 2, but their balances were growing, reflecting the overall expansion of banks’ balance sheets. Their average liquidity-generating capacity is reported in column “liquidity” of the table. The capacity is consistent with the liquidity weights used to compute the regulatory liquidity ratio of each bank, i.e., the Liquidity Coverage Ratio. The liquidity weights allow us to proxy a price impact of the transacted securities and, consequently, to parameterize the inverse demand functions f_m of the model. Finally, BCAR is used to extract information about banks’ capital levels.

	Balance sheet item	Volume		Return		Volatility		Liquidity
		mean	sd	mean	sd	mean	sd	
L	loans	37.2	17.2					
C0	cash	6.9	8.3	0.155	0.057	0.219	0.030	100
S0.0	Agency MBS	1.8	1.6	0.541	0.020	0.692	0.024	100
S0.1	HR Gov securities	8.9	2.8	0.635	0.027	0.707	0.029	100
S0.2	LR Gov securities	0.4	0.7	0.591	0.041	0.770	0.038	50
S0.3	MR Gov securities	1.0	0.7	0.560	0.052	0.626	0.039	85
S1.1	Equity Financial	3.6	2.5	0.692	0.059	0.698	0.024	0
S1.2	Equity Non-financial	7.6	2.6	0.768	0.035	0.743	0.024	0
S2.1	Financial Debt (ABS/ABCP and Corp. Bonds)	10.3	13.4	0.745	0.094	0.774	0.068	0
S2.2	HR Corporate Bonds (non-financial)	3.0	6.4	0.719	0.073	0.790	0.046	85
S2.3	LR Corporate Bonds (non-financial)	6.2	8.5	0.754	0.083	0.793	0.059	0
S2.4	MR Corporate Bonds (non-financial)	1.9	1.9	0.750	0.068	0.859	0.040	50
S2.5	Other securities	2.2	2.4	0.721	0.090	0.726	0.066	50
S2.6	RMBS Uninsured	0.5	0.9	0.646	0.082	0.714	0.041	0
S3.0	RevRepo – Agency MBS	6.0	10.6	0.238	0.104	0.110	0.006	0
S3.1	RevRepo – Financial Debt (Corp Bonds, ABS/ABCP)	1.2	2.2	0.271	0.113	0.105	0.009	43
IA	Interbank assets	1.5	1.5					
IL	Interbank liabilities	2.7	2.0					
F0	Retail deposits	40.0	1.8					4.3
F0.0	Secured wholesale funding	18.2	4.1					24.5
F0.1	Unsecured wholesale and corporate deposits	34.1	3.4					50.0
E0	Capital	3.6	0.3					

Table 1: Statistics of data used to parameterize the model. All numbers in % based on time series of quarterly data between 2015-06-30 and 2018-12-31.

“Volume” – in percent of the average total assets of the D-SIBs;

“Return” – average quarterly return on assets;

“Volatility” – risk of return on the assets;

“Liquidity” – liquidity weights reported for the calculation of the Liquidity Coverage Ratio (expected cash to be generated by assets for asset classes and run-off rates for liabilities);

“Mean” – average across banks and periods; “sd” – time average of standard deviations across banks for a given data.

To complete the modelling of our system, we consider a few additional assumptions. First, we assume, as in Greenwood et al. (2015), linear inverse demand functions with a 10 basis point impact from liquidations of 10 billion dollars of exposure as a benchmark that is scaled proportional to the liquidity weights, i.e., the higher the “1-weight,” the higher the price impacts of a transaction. The weights are reported in Table 1. Second, we set the volatility of returns on assets that feed into the risk matrix C based on the average (across reporting banks) historical volatility of returns on those instruments. We assume that the risk matrix is

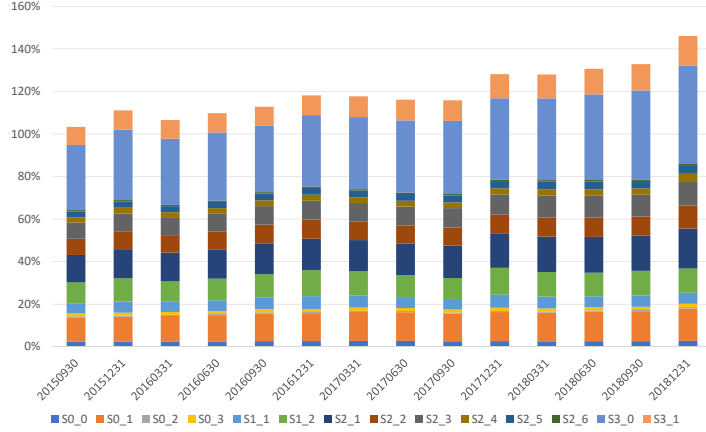


Figure 2: Evolution of the potential liquidity buffer, i.e., liquid and less liquid assets, measured as the average (across banks) share of a given asset category in the total pool of liquid and less liquid assets.

diagonal, i.e., there are no correlations between assets. The returns are calculated based on a time series of information contained in the P3 OSFI returns and normalized by corresponding exposures that are reported in M4 returns. The volatilities are presented in Table 1.

Finally, the risk aversion parameter γ and the fractions β of asset revaluation recognized as losses are calibrated using equation (5). We are looking for bank- and period-specific values of γ and β such that the theoretically optimal bank asset structure is the closest to the observed one. The detailed outcomes of calibration are shown in the Appendix.

4.2 Numerical stress tests and simulations

We illustrate our model from Section 2 by conducting a set of simulations to determine how banks would (theoretically) react to funding shocks. Specifically, we consider two classes of funding shocks:

1. *Common shocks*: All the banks experience a funding shock of the same magnitude, i.e., the same percentage outflow in a given funding category. This shock mimics a general market distress.
2. *Idiosyncratic shocks*: Only one bank experiences a funding shock and other banks only react to the management actions of the initially stressed bank. This shock mimics a situation of loss of trust to one bank that may be related to its deteriorated financial conditions.

We assume that in both classes of shocks it is unsecured wholesale and corporate funding that is in distress. These sources of funding are in general sensitive to the market conditions of banks' financial

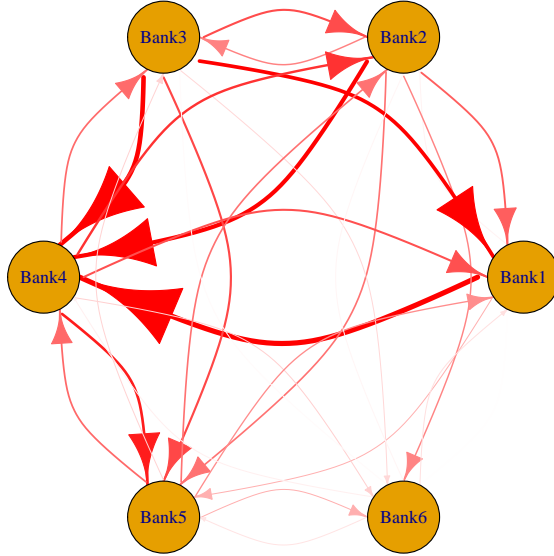


Figure 3: Network of interbank exposures in which nodes indicate banks, the width of edges and intensity of the colour are proportional to a square root of the exposures, and arrows indicate the direction of exposures, i.e., an arrow from Bank i to Bank j tells that bank i is exposed to risk related to interbank lending, debt instruments or derivatives from bank j .

standing. For illustration, we consider several shock scenarios. Specifically, we analyze run-off shocks on a grid of percentage outflows $\{10\%, 20\%, \dots, 50\%\}$; in each scenario the magnitude is equal across all shocked banks, thus describing either a system-wide funding shock or the severity of how a given bank's funding conditions deteriorate. We apply those shocks to all the snapshots of data in the sample but – to be concise – we are selective in the presentation of only representative snapshots of results for detailed discussion and conclusions. Additionally, we also explore extremely severe scenarios of shocks above 70% run-off rates to explore the default contagion mechanism in the model. For shocks of this very high magnitude, some of the banks in the sample would not have sufficient assets to liquidate to meet their obliged payments. Notably, this extremely severe event is highly unlikely to materialize, thus this type of simulation is only to illustrate the default contagion channel in the model.

We solve the model by running Algorithm 2.6 with $\epsilon = 0.01$ liquidation step for 1000 iterations of the tâtonnement process. We report the evolution of prices that are a harmonized metric of distress. Below, we report some observations regarding our model and this dataset regarding, e.g., convergence, dependence of price impact on the shock size, and the dynamics of vulnerabilities.

4.2.1 Convergence

Asymptotic behaviour of Algorithm 2.6 indicates the observed post-stress response of the market; for some assets, this convergence means an oscillation of prices within a narrow band. In Figure 5, we show the behaviour of prices in one specific example of the shock (50%) and one snapshot of data (2018-12-31).

First, the process converges after 100 steps of the (discretized) tâtonnement process as the curves representing prices and cash holdings flatten out.

Second, revaluation of assets differs across asset classes, with one asset repriced by more than 1%.²

Third, two asset categories converge to a set of prices within which they fluctuate, though the fluctuations are in a tight band. This phenomenon suggests that our modelling framework generates endogenous noise in the prices without any exogenous randomness in the model and predicts varying volatilities.

Fourth, the tâtonnement fluctuates more in the case of an idiosyncratic shock than in the case of the common shock – even though the impact of the shock on prices is more contained (see Figure 6). There is more randomness in prices as they converge, which is created by buyers and sellers of assets responding in different directions to changes in prices. Common market shocks cause a rather unidirectional response of the banks, consistently depressing prices towards equilibrium.

Implicitly, the dynamics of the market after an idiosyncratic shock can also be interpreted as trading between two sides of the market. Banks not hit by the initial funding outflow would buy assets from the banks fire-selling to supplement liquidity. However, in our setup we cannot distinguish pairs of transacting banks. Models of market matching can address this issue (see, e.g., Cui and Radde (2019)), but we are focused not on the trading patterns but rather on the impact of trading on market prices.

4.2.2 Price impacts as a function of shock size

The magnitude of funding shocks matters for the prices of assets in equilibrium. Intuitively, small shocks do not instigate contagion, with prices remaining intact since banks have enough cash to cover the run-offs. This is illustrated in Figures 7 and 8, with the straight top line corresponding to a 10% outflow of unsecured wholesale funding. As the magnitude of shock increases (from 10% to 50%), prices start to react after banks' reallocation of assets. The systemic impact grows disproportionately to the initial shock. This can be seen in the widening distance between lines in Figure 7 and is a manifestation of the nonlinearities related to the contagion process we model. Notably, nonlinearity arises even though the price impact function assumed in this case study is linear.

Since the sensitivities of asset prices to the transacted volumes of assets are the key parameter of the

²For confidentiality reasons, we cannot report more detailed output of the simulations in the current version of the paper.

model to capture the indirect channel of contagion, we run an additional experiment to study how the results of the simulations depend on those sensitivities. We select one snapshot in the data (the most recent observations, 2018-12-31), apply a common shock of 25% outflow of unsecured wholesale and corporate funding, and gradually and proportionally increase the sensitivities of asset prices. We apply multipliers in $[1,2]$. The outcomes of Algorithm 2.6 are shown in Figure 17. Higher sensitivity of prices to transacted volumes translates into larger decreases in the prices of assets under the funding shock. However, sensitivity of prices in equilibrium vary across assets – some prices drop as much as 300 percentage points as the sensitivity grows two times; other prices move only by a few basis points.³

4.2.3 Market regulator

One important caveat to the conclusions about price impact is related to the absence of a market regulator in the simulations. Market regulators like central banks have their mandate to watch market liquidity and restore it if it is impaired.⁴ This power was demonstrated, for instance, right after the unexpected outbreak of the COVID-19 pandemic, which impacted market and funding liquidity in March and April, 2020; in that period, the market turmoil prompted central banks around the world to inject liquidity into the financial system and to roll out special liquidity facilities (Cavallino and Fiore, 2020). However, there is usually a reaction time that implies initial sell-off of assets and market liquidity dislocation, especially in the case of such an unprecedented shock as COVID-19 (Haas and Neely, 2020). Our model can provide insights into this period of a crisis, when policy support measures are still being customized and deployed.

Still, our framework is general enough, allowing us to embed a market regulator. The only requirement is that the regulator’s actions can be formulated in terms of an optimization program. We illustrate its role in the system assuming that the regulator would try to strategically minimize the price impact of banks’ transactions following a shock. This is consistent with, for instance, central banks’ role to maintain price stability and favourable liquidity conditions on the market.

Specifically, we add node $N + 1$ to the model representing the regulator. We formulate the regulator’s preferences as deviation of prices from the initial price equal to 1. We assume that the regulator could buy and sell assets but only of a certain credit quality, denoted by an eligibility subset $Q \subset \{1, 2, \dots, M\}$. Without loss of generality, we can assume that the regulator does not hold any assets at the start of the funding shock, which means that its strategy y represents net purchasing if it is positive and selling for

³Additionally, we run sensitivity of the equilibrium prices to changes in the calibrated parameters of risk aversion (γ) and mark-to-market fraction of banks’ portfolios (β). Corresponding figures are included in the Appendix (Figures 18 and 19).

⁴See for instance the framework of the Bank of Canada (<https://www.bankofcanada.ca/markets/market-operations-liquidity-provision/>) or ECB (<https://www.ecb.europa.eu/mopo/liq/html/index.en.html>).

negative values of y . Mathematically, the utility of the regulator is written down as

$$u_{N+1}(y) = \left\| f \left(\sum_{i=1}^{N+1} [(x_i - y_i)] \right) - \bar{1} \right\|^2. \quad (6)$$

Moreover, the regulator has a budget constraint limiting its self-imposed size of the balance sheet (dollar amount B). Combining the budget constraint and eligibility of assets transacted by the regulator, we can write down the admissible set of actions as

$$\mathcal{A}_{N+1}(q) = \left\{ y_{N+1} \in \mathbb{R}^M \mid \sum_{m=1}^M q_m y_{im} \leq B, \quad y_{im} = 0 \quad \text{if } i \notin Q \right\}. \quad (7)$$

The regulator maximizes its utility subject to other banks' holding of assets, i.e., $u_{N+1}(y_{N+1}, (y_1^*, \dots, y_N^*))$, over $\mathcal{A}_{N+1}(q)$. Notably, since the regulator is represented as another node in the modelled system, the commercial banks $1, \dots, N$ consider the actions of the regulator in their strategic decisions about selling or buying of assets.

For simplicity, the regulator is not present on the interbank market of direct lending and borrowing; therefore, it is excluded from the interbank network and, thus, the clearing payments algorithm. This assumption would not materially reduce the generality of the model since the regulator would in any case not be expected to default.

In such an augmented setup, we run a sequence of simulations that illustrate the impact of the regulator on the prices of assets in equilibrium. Specifically, we assume B is large enough, so that the regulator allows for unlimited expansion of its balance sheet. Then, we link a composition of Q with the haircuts of the assets, i.e., we parameterize $Q(h)$ as follows:

$$Q(h) = \{m \in \{1, \dots, M\} \mid \text{liquidity}_m < h\}, \quad (8)$$

where liquidity_m is a liquidity parameter of asset class m presented in Table 1. We assume a uniform funding shock across banks equal to a 25% run-off rate of the unsecured funding sources.

The results are illustrated in Figure 4. We can clearly see that the prices in equilibrium in general increase with the number of assets eligible in the transactions executed by the regulator. Point 0 on the horizontal axis of the figure corresponds to the case of no regulator of the market. Then, for instance, point 20 refers to a case where the regulator transacts only assets that have liquidity weight lower than 20. Notably, the highest impact of the increase of the pool of eligible assets for transactions with the regulator occurs when the regulator enters the market (the threshold haircut increases from 0 to some positive number). In other

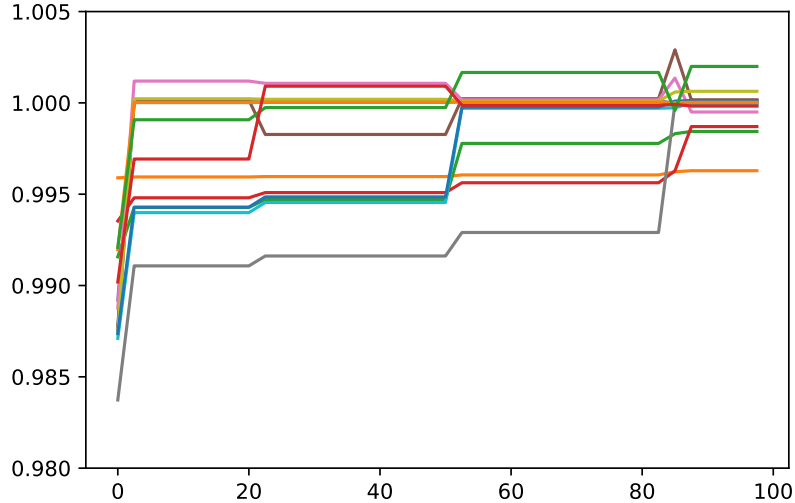


Figure 4: Prices of assets in the equilibrium with active market regulator given a shock corresponding to a 25% run-off rate of the unsecured wholesale funding affecting all six banks. The x-axis shows the threshold haircut of assets accepted by the regulator (i.e., assets that the regulator is willing to buy or sell); the y-axis shows asset prices (colours represent different assets classes).

words, the regulators start to buy or sell the highest quality assets to stabilize their prices. Those assets would be the preferred sources of liquidity for banks.

4.2.4 Strategic interactions

In convergence to the optimal structure of balance sheets, banks consider other banks' portfolio management actions in their optimization program. Therefore, we are looking at banks' best responses to other banks' moves; the equilibrium we consider combines a clearing payments vector on the interbank market and optimal transactions of assets held in liquidity buffers. For each bank, the optimization of its peers is prescribed in the utility functions through the price impact, which assumes that each bank optimizes its assets subject to funding shock and observed movements in asset prices. To do so, each bank has a perfect insight into other banks' portfolio structures so that it can consider the aggregate transacted volumes $\sum_{j=1}^N [x_j - y_j]$. Alternatively, we can expect that exact management actions of other banks are opaque and banks only see the changes in prices. In such a case, banks would only consider their own impact on the market, i.e., bank i analyzes the impact of its transacted volumes $x_i - y_i$ to optimize asset holdings y_i . We look at the implications of the prices in equilibrium of such a myopic optimization. We show the corresponding dynamic of prices in the tâtonnement process in Figure 16.

Remark 4.1. Though we formulate the utility functions *without* strategic interactions so that the clearing

solutions would, mathematically, provide Nash equilibria, we do *not* consider such a setting as providing Nash equilibrium. Specifically, the modified utility function for bank i is given by $u_i(\cdot, x_{-i})$ where u_i is defined in Section 3 rather than $u_i(\cdot, y_{-i})$ for strategic interactions; this distinction is introduced due to the partial information available to the banks without strategic interactions. As the banks would ultimately wish to optimize the setting *with* strategic interactions, they may be able to modify their strategy y_i in order to improve the *true* utility (when fixing all other banks' actions y_{-i}).

Three observations can be made on the reaction and overreaction of bank strategies. First, banks that are optimizing balance sheets in isolation will depress asset prices more than if they were strategically interacting with other banks. We conjecture this is because the “isolated” banks do not internalize other banks' potential actions causing additional pressures on the prices of assets; with interactions the banks may sell less, which corresponds with higher marginal cash raised from any liquidation. Second, banks are less likely to “overreact” in a flight to safety, i.e., sell more assets than strictly necessary, when taking other banks' actions into account. This can be measured by considering the cash held (a_i^*), which (1) can be computed from the surplus from the budget constraint if the bank is solvent and (2) is equal to the assets if the bank is insolvent; we compute and display this cash accumulation (as a fraction of total assets) in Figure 20. Third, endogenous volatility and the oscillation of prices are much smaller when banks decide on rebalancing and cash-raising policies in isolation. This can be seen by comparing Figures 5 and 16.

We conjecture that these observations will generally hold since all banks have the same utility function (up to parameter differences) and, thus, all seek to liquidate similar assets. Therefore, when considering the utility function with full interactions, we find that each institution, by endogenizing the impacts from other banks, internalizes the trade-offs in what it is selling. Strategic responses of banks to other banks' moves make the more frequently traded assets fluctuate more, which creates market volatility. In contrast, without interactions, each institution does what is locally optimal for it, which can make the system worse off. However, the fluctuations of prices are less pronounced. Conversely, when considering strategic interactions, banks are more prone to initially overreact and accumulate cash since banks consider that the value of assets – and, in turn, the capacity of their balance sheets to raise cash – can be impaired by the collective actions of the whole system of banks. Figure 20a shows that cash initially increases more with interactions than without them and then declines below the accumulated cash with banks optimizing their balance sheets in isolation, presented in Figure 20b. All in all, there appears to be a trade-off between price impacts and the volatility of prices, as seen by comparing and contrasting the utility with strategic interactions to the utility without interactions.

4.2.5 Default contagion

The network model presented in Section 2 also allows for the analysis of the effects of shocks through the network of obligations. This network transmits distress between banks once institutions default and fail to pay back their obligations to other banks in full because they hold insufficient resources. Herein, we look at the relationship between shock size and the ability of banks to pay back their obligations to other banks. To do so, we apply a range of shocks to the unsecured wholesale funding sources and repo funding.⁵ The fraction of liabilities paid in the clearing payment equilibrium is presented in Figure 9. First, only for very severe shocks – beyond 85% of the unsecured funding volumes – do any banks have insufficient liquid assets to satisfy their creditors. However, the clearing payments fall sharply for increasing run-off rates past the (bank-specific) default threshold. Second, the sensitivity of payments in equilibrium to the funding shock differs substantially across banks.

Furthermore, we can quantify the impact of partial payments by one bank on its creditors’ ability to pay debts. To allow for comparability across banks, this significance can be measured as a fraction of creditors’ capital. Specifically, we define the measure for bank i as

$$m_i := \sum_{j=1}^N \pi_{ji} (\bar{P}_j - p_j^{(\infty)}) / c_i.$$

Even for the most severe shocks (100% run-off rate), the unpaid interbank liabilities range between 0.6% and 3.2% of banks’ capital (see Table 2). Though small, this impact is not negligible and amounts to CAD 10–60 billion.

Losses related to direct exposures of banks to other banks are significantly smaller than those incurred through the revaluation of assets following the rebalancing of the portfolios. Figure 11 shows that interbank contagion can only generate losses as much as 0.1% of the total assets in the banking system and only in the very extreme stress scenario. On the contrary, fire sales of assets are substantial even for a moderately severe scenario of 50% run-off rate on the unsecured funding and can bring losses of 1% of assets in this case. This is implied by a relatively thin interbank layer in the modelled banking system. The prevailing role of the price-mediated contagion channel is consistent with findings of Greenwood et al. (2015) and Calimani et al. (2019).

Defaults on interbank payments can occur endogenously in the model as a result of declining valuation of banks’ assets. Banks respond to the shocks by selling assets, which reduces their prices and, consequently their capacity to create liquidity. Even though the initial shock allows banks to pay back their liabilities

⁵No run-off rate for the unsecured funding volumes created a default event. Therefore, for illustration purposes we considered an extended set of funding sources in distress.

when asset prices are 1, the equilibrium prices may not. It is illustrated in Figure 12. Most of the banks hit by a funding shock from a bank-specific range would only default on payments after a number of steps in the tâtonnement process.

4.2.6 Dynamics of vulnerabilities

Given the time series of data we analyze, we additionally consider the evolution of prices in equilibrium for a specific shock size. We chose a run-off rate of 50% and illustrated the differences in equilibrium prices, i.e., subtracting equilibrium prices at the starting date 2015-06-30. The output is shown in Figures 13 and 14. In case of the common shock, there are two regimes. First, until 2017-09-30 the impact is very limited and stable (with one outlier for 2015-12-31). After 2017-12-31, the impact of the same shock steadily increases. This may suggest that banks become more vulnerable to funding shocks given their reliance on unsecured wholesale funding. In the case of an idiosyncratic shock, assets form two distinctive groups; in one group prices consistently drop, in the other prices increase. This may reflect the compensating effects on prices created by banks that are not forced to liquidate assets since they are not hit by the funding shock.

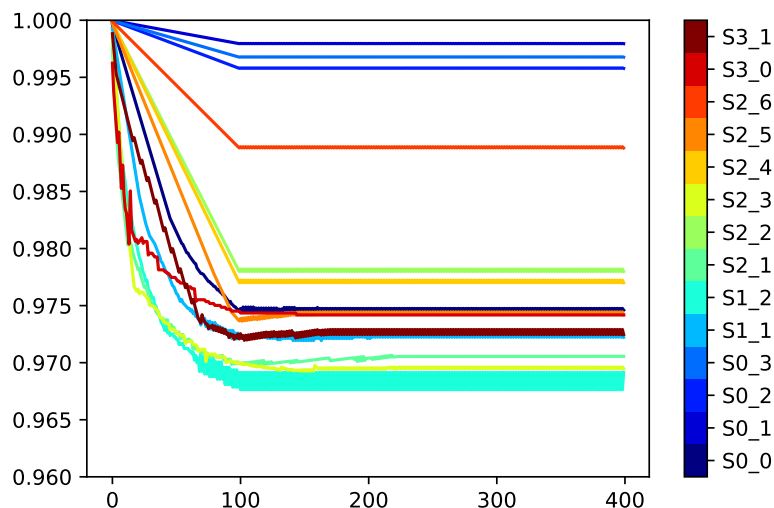


Figure 5: Prices of assets (y-axis) in the steps (x-axis) of the tâtonnement process searching for the equilibrium (system-wide funding shock) given a shock corresponding to a 50% run-off rate of the unsecured wholesale funding affecting all six banks. Time is measured in the steps of the tâtonnement process and prices are normalized to 1 at the start of the algorithm.

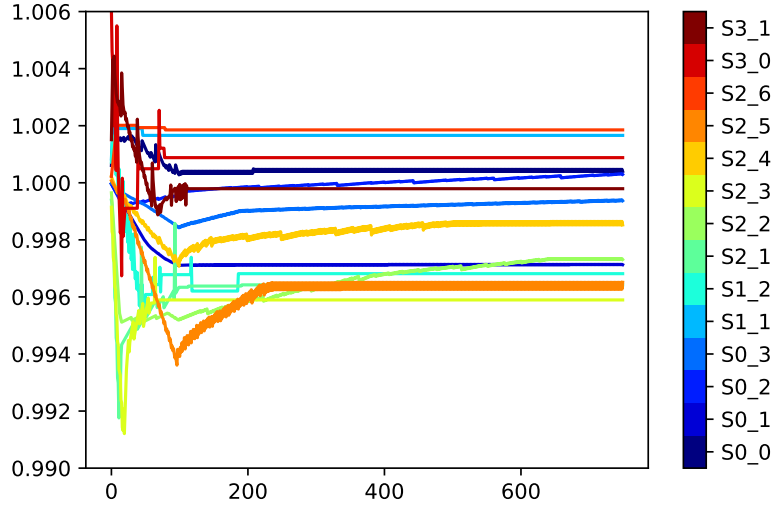


Figure 6: Prices of assets (y-axis) in the steps (x-axis) of the tâtonnement process searching for the equilibrium (idiosyncratic funding shock) given a shock corresponding to a 50% run-off rate of the unsecured wholesale funding affecting one bank. Time is measured in the steps of the tâtonnement process and prices are normalized to 1 at the start of the algorithm.

	B1	B2	B3	B4	B5	B6
m	0.6	2.1	0.9	3.2	2.1	1.1

Table 2: Potential losses on exposures to banks defaulting on their payments (% of banks capital) under extremely severe scenario of 100% shock to unsecured wholesale and corporate funding.

5 Conclusions

A decade after the Global Financial Crisis, systemic risk is still not fully understood. Systemic risk is attributed to complex structures of financial system and management actions of financial agents that may have unpredictable consequences. We shed light on some aspects of systemic risk related to network effects in the interconnected interbank market and asset management under stress.

To this end, we build a model of the interbank market where banks are linked by direct exposures and may respond to financial shocks by rebalancing their assets to raise cash and maximize utility from investment opportunities. We bring the model to the data on the Canadian interbank market of domestically significant banks. This allows us to measure financial vulnerabilities related to funding shocks.

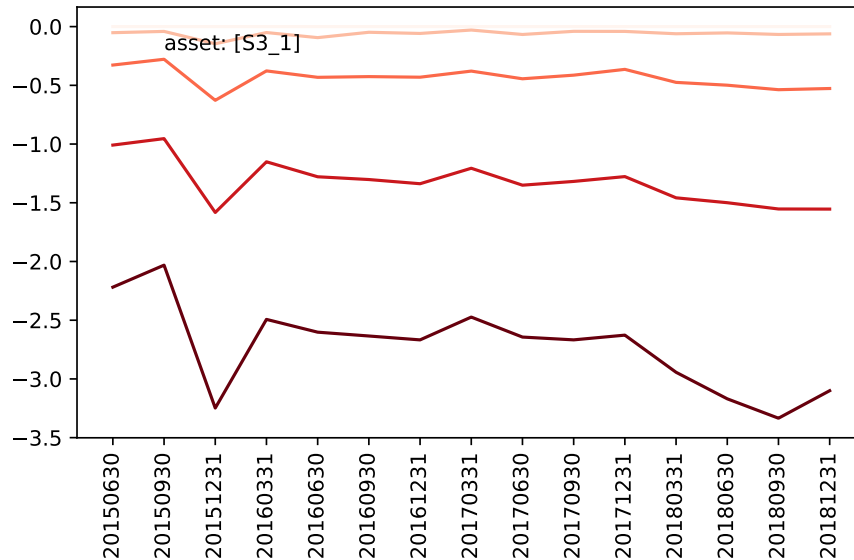


Figure 7: Time series of price impacts (in pp) of a single asset class (S3_1) in equilibrium after a shock to unsecured funding to all six banks. Each colour represents a magnitude of the shock (the darker the stronger the shock; from 0% to 75%).

Acknowledgements

We would like to thank an anonymous referee, Ruben Hipp, Banff International Research Centre, Tom Hurd, and participants of Analytical Methods for Financial Systemic Risk workshop (Banff), as well as participants of a research seminar of the Bank of Canada for comments and Nicolas Whitman for excellent research assistance.

References

- Amini, H., Filipović, D. and Minca, A. (2016), ‘Uniqueness of equilibrium in a payment system with liquidation costs’, *Operations Research Letters* **44**(1), 1–5.
- Banerjee, T. and Feinstein, Z. (2019), ‘Impact of contingent payments on systemic risk in financial networks’, *Mathematics and Financial Economics* **13**(4), 617–636.
- Banerjee, T. and Feinstein, Z. (2020), ‘Price mediated contagion through capital ratio requirements’. Working Paper.
- Braouezec, Y. and Wagalath, L. (2019), ‘Strategic fire-sales and price-mediated contagion in the banking system’, *European Journal of Operational Research* **274**(3), 1180–1197.

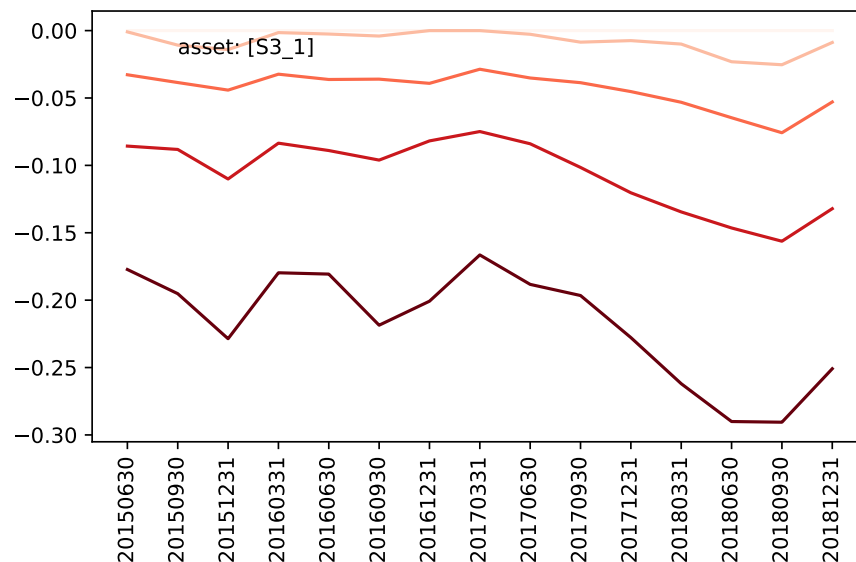


Figure 8: Time series of price impacts (in pp) of a single asset class (S3.1) in equilibrium after a shock to unsecured wholesale and corporate funding of one bank. Each colour represents a magnitude of the shock (the darker the stronger the shock; from 10% to 50%)

Braverman, A. and Minca, A. (2018), ‘Networks of common asset holdings: aggregation and measures of vulnerability’, *Journal of Network Theory in Finance* pp. 53–78.

Caballero, R. J. and Simsek, A. (2013), ‘Fire sales in a model of complexity’, *The Journal of Finance* **68**(6), 2549–2587.

Calimani, S., Hałaj, G. and Zochowski, D. (2019), ‘Simulating fire sales in a system of banks and asset managers’, *Journal of Banking & Finance* p. 105707.

Cavallino, P. and Fiore, F. D. (2020), ‘Central banks’ response to Covid-19 in advanced economies’, BIS Bulletin 21, Bank of International Settlements.

Cifuentes, R., Ferrucci, G. and Shin, H. (2005), ‘Liquidity risk and contagion’, *Journal of the European Economic Association* **3**(2/3), 556–566.

Cont, R. and Schaanning, E. (2019), ‘Monitoring indirect contagion’, *Journal of Banking & Finance* **104**, 85–102.

Cui, W. and Radde, S. (2019), ‘Search-based Endogenous Asset Liquidity and the Macroeconomy’, *Journal of the European Economic Association* .

Duarte, F. and Eisenbach, T. (2018), ‘Fire-sale spillovers and systemic risk’, *Federal Reserve Bank of New York Staff Reports* .

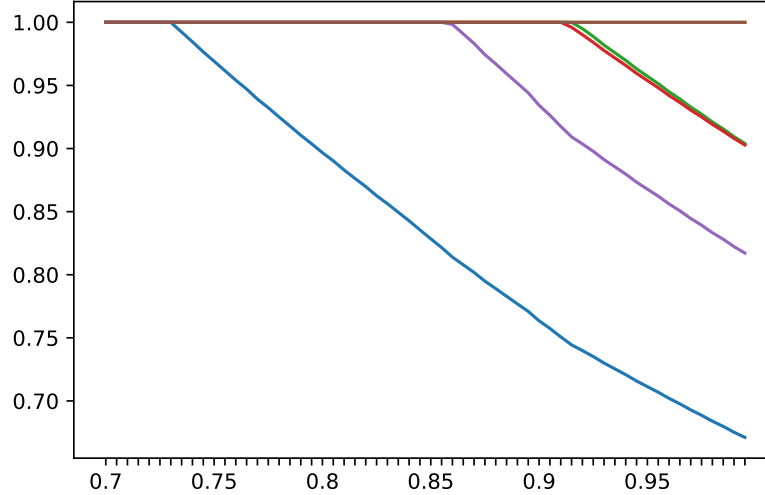


Figure 9: Clearing payments p^* (as a fraction of required payments \bar{P}) in equilibrium for different magnitudes of funding shocks, i.e., the run-off rate of the unsecured wholesale funding and corporate term deposits (the same magnitude for all banks, x-axis). Each line corresponds to a bank.

Eisenberg, L. and Noe, T. (2001), ‘Systemic risk in financial systems’, *Management Science* **47**(2), 236–249.

Feinstein, Z. (2017), ‘Financial contagion and asset liquidation strategies’, *Operations Research Letters* **45**(2), 109–114.

Feinstein, Z. (2019), ‘Obligations with physical delivery in a multi-layered financial network’, *SIAM Journal on Financial Mathematics* **10**(4), 877–906.

Feinstein, Z. (2020), ‘Capital regulation under price impacts and dynamic financial contagion’, *European Journal of Operational Research* **281**(2), 449–463.

FSB (2016), *Implementation and Effects of the G20 Financial Regulatory Reforms*, Financial Stability Board.
URL: <https://www.fsb.org/wp-content/uploads/P161019.pdf>

FSB (2020), ‘COVID-19 pandemic: Financial stability implications and policy measures taken’, Working paper, Financial Stability Board.

Gouriéroux, C., Héam, J.-C. and Monfort, A. (2012), ‘Bilateral exposures and systemic solvency risk’, *Canadian Journal of Economics* **45**(4), 1273–1309.

Greenwood, R., Landier, A. and Thesmar, D. (2015), ‘Vulnerable banks’, *Journal of Financial Economics* **115**(3), 471–485.

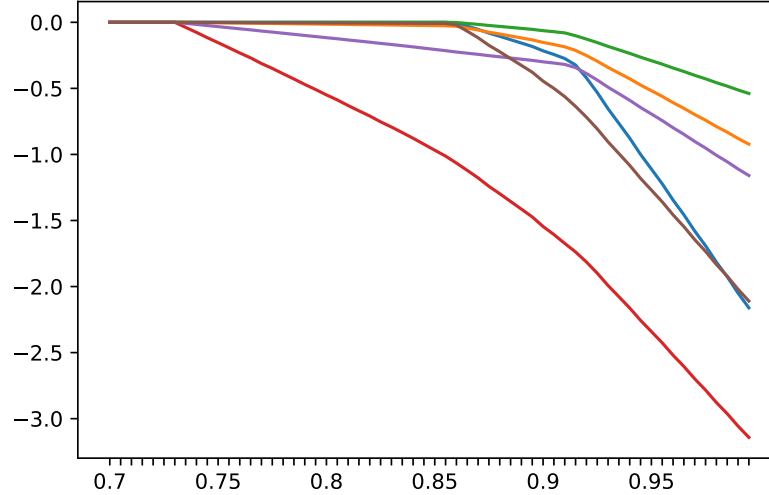


Figure 10: The impact of defaulted payments on bank creditors (in % of capital), i.e., the losses incurred by banks as a result of creditors' defaults on their interbank obligations, as a function of the run-off rate of the unsecured wholesale funding and corporate term deposits (the same magnitude for all banks, x-axis). Each line corresponds to a banks.

Haas, J. and Neely, C. (2020), 'Central bank responses to COVID-19', Economic Synopsis 23, Federal Reserve Bank of St. Louis.

Klages-Mundt, A. and Minca, A. (2020), 'Cascading losses in reinsurance networks', *Management Science* . DOI: 10.1287/mnsc.2019.3389.

Rogers, L. C. and Veraart, L. A. (2013), 'Failure and rescue in an interbank network', *Management Science* **59**(4), 882–898.

Schuldenzucker, S., Seuken, S. and Battiston, S. (2019), 'Default ambiguity: Credit default swaps create new systemic risks in financial networks', *Management Science* **0**(0). DOI: 10.1287/mnsc.2019.3304.

Shleifer, A. and Vishny, R. (2011), 'Fire sales in finance and macroeconomics', *Journal of Economic Perspectives* **25**(1), 29–48.

Suzuki, T. (2002), 'Valuing corporate debt: the effect of cross-holdings of stock and debt', *Journal of Operations Research* **45**(2), 123–144.

Weber, S. and Weske, K. (2017), 'The joint impact of bankruptcy costs, fire sales and cross-holdings on systemic risk in financial networks', *Probability, Uncertainty and Quantitative Risk* **2**(1), 9.

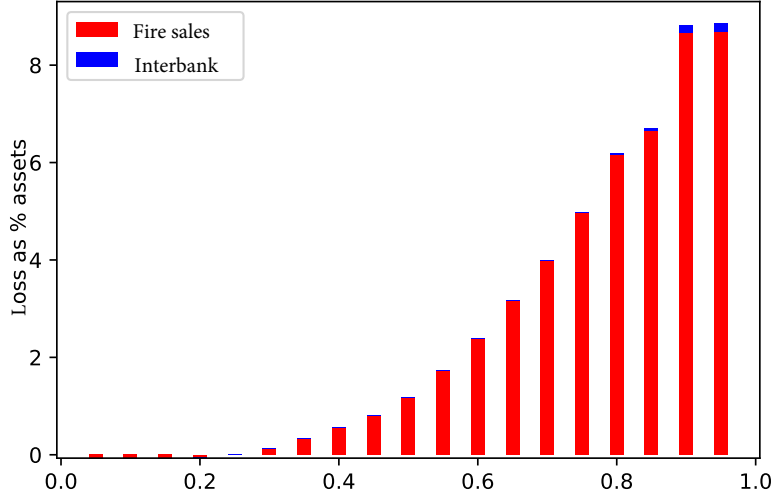


Figure 11: Decomposition of losses into fire sale losses and interbank contagion losses (as % of total assets) after a run-off shock to the unsecured wholesale funding and corporate term deposits (the same magnitude for all banks).

	B1	B2	B3	B4	B5	B6
mean	0.008	0.007	0.006	0.003	0.005	0.010
std	0.0017	0.0009	0.0006	0.0001	0.0001	0.0010

Table 3: Calibrated risk aversions.

A Appendix

A.1 Calibration

To assess the accuracy of the calibration, we compare the observed composition of banks' assets with the asset structures obtained in the portfolio optimization using the calibrated values of risk aversion γ and mark-to-market elasticity β . On the whole, banks' total assets are recomputed from the calibrated values of risk aversion, and mark-to-market elasticities are very close to the observed values. On average, total assets in calibration are 96% of the observed total assets (average across banks and periods), with only a 1.6% standard deviation. However, there is more divergence between calibrated and observed asset structures. We measure the accuracy of the calibrated asset structures by the normalized difference between the observed and calibrated assets. The measures for each bank and for all points in time in the data sample are presented in Figure 15. The accuracy is generally between 5% and 20%, with one bank around 30%.

A.2 Additional simulations

asset	B1	B2	B3	B4	B5	B6
S3.1	98	64	79	98	99	92
S3.0	96	66	89	97	97	94
S2.6	97	49	50	95	87	72
S2.5	92	51	69	94	89	92
S2.4	94	66	89	50	99	96
S2.3	94	75	88	97	95	89
S2.2	93	79	87	93	96	99
S2.1	92	37	72	96	97	92
S1.2	97	49	87	94	93	99
S1.1	99	52	73	98	96	96
S0.3	99	52	81	95	99	99
S0.2	99	53	50	50	50	50
S0.1	99	94	97	99	99	99
S0.0	99	89	86	99	99	97

Table 4: Calibrated mark-to-market elasticity (in %) averaged for all time points in the data.

asset	B1	B2	B3	B4	B5	B6
S3.1	2	3	16	1	0	1
S3.0	1	12	7	1	0	0
S2.6	3	2	0	6	11	8
S2.5	5	1	13	3	8	2
S2.4	3	4	8	0	1	3
S2.3	3	2	6	1	1	4
S2.2	3	1	7	0	1	0
S2.1	6	10	10	3	2	2
S1.2	3	1	8	0	1	0
S1.1	1	4	17	2	3	1
S0.3	1	4	15	1	0	0
S0.2	0	3	0	0	0	0
S0.1	0	1	2	0	0	0
S0.0	0	2	10	0	0	2

Table 5: Dispersion of calibrated mark-to-market elasticity (in %), i.e., the standard deviation of calibrated parameters for all the time points in the data.

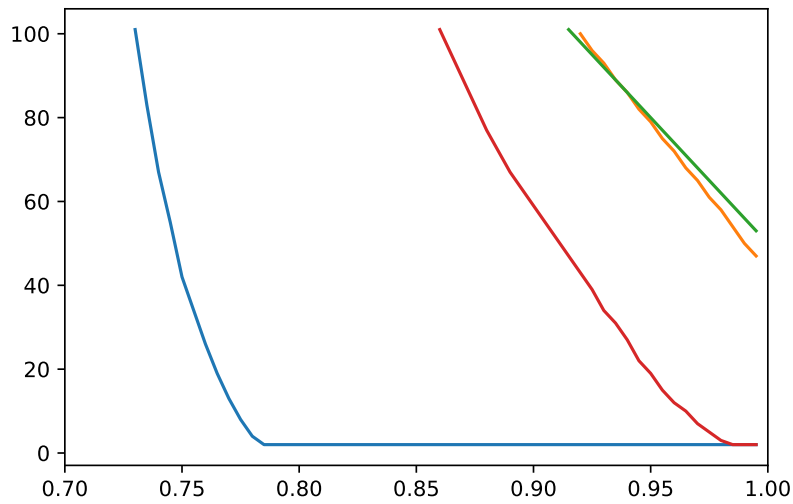


Figure 12: The first step in the (discretized) tâtonnement process in which banks default on payments as a function of the magnitude of the shock. Values larger than 1 indicate that defaults occur due to the endogenous decline of the value of pool of assets that can be used to counterbalance the initial funding shock. Each line represents a bank.

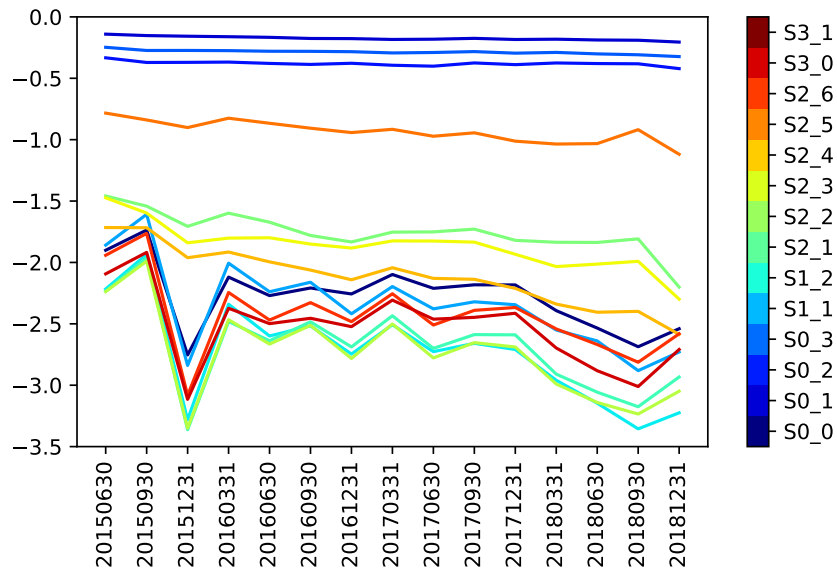


Figure 13: Time series of price impacts (in pp) of all assets for a given period measured as the difference between prices in equilibrium at [yyyymmdd] with the starting point of 2015-06-30 given a 50% shock to unsecured funding to all banks. Each colour represents one asset.

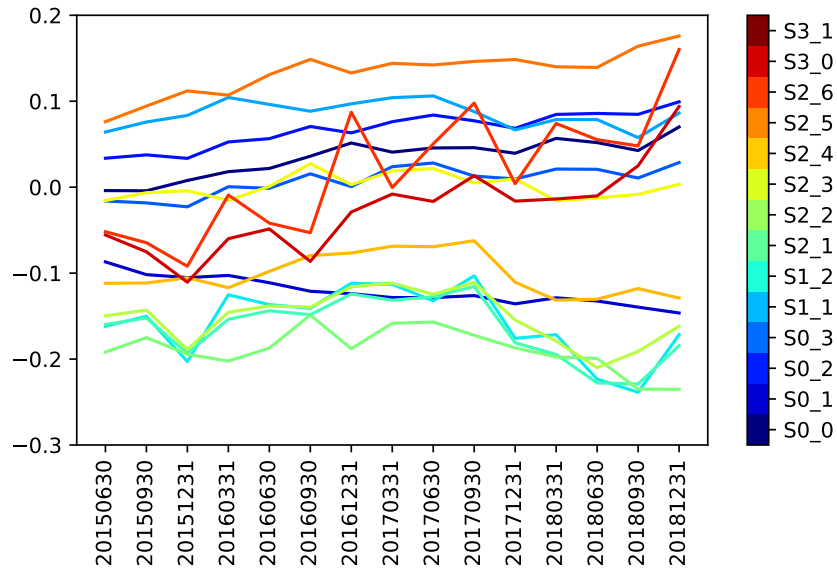


Figure 14: Time series of price impacts (in pp) of all assets for a given period measured as the difference between prices in equilibrium at [yyyymmdd] with the starting point of 2015-06-30 given a 50% shock to unsecured funding of one bank (i.e., an idiosyncratic shock). Each colour represents one asset.

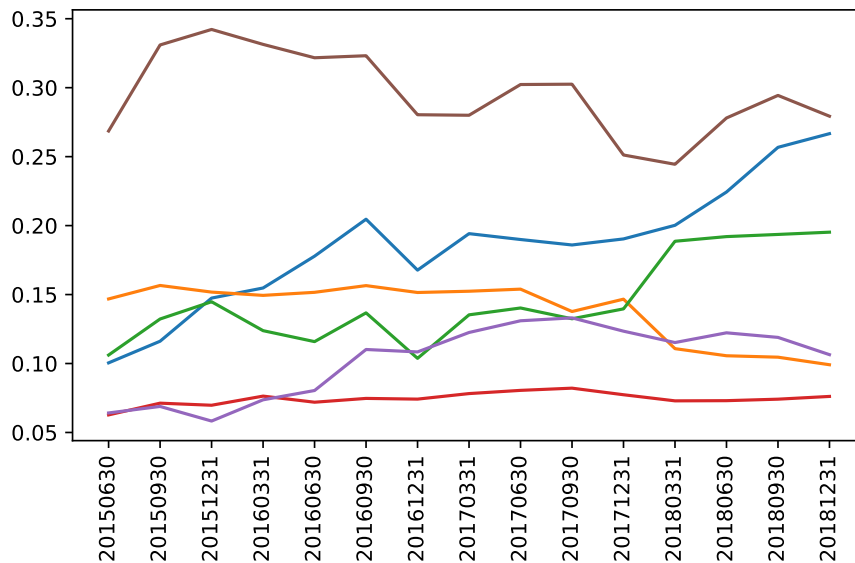


Figure 15: Accuracy of the calibration measured by the l^1 -norm of the difference between the calibrated assets and observed assets (normalized by the observed total assets of the bank). Each line represents a bank.

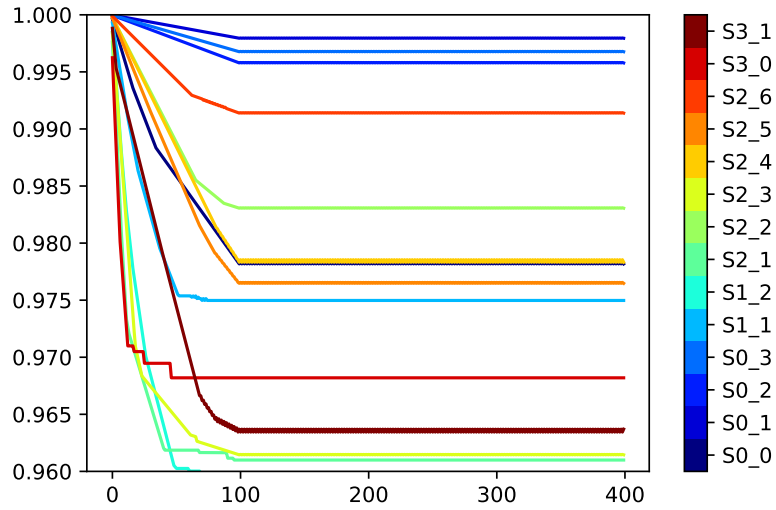


Figure 16: Prices of assets (y-axis) in the discretized steps (x-axis) of the tâtonnement process. Prices are normalized to 1 at the start of the process. Funding shock is applied through a 50% run-off rate of the unsecured wholesale funding to all banks assuming that banks do not internalize other banks' management actions in their optimal choice of asset structures.

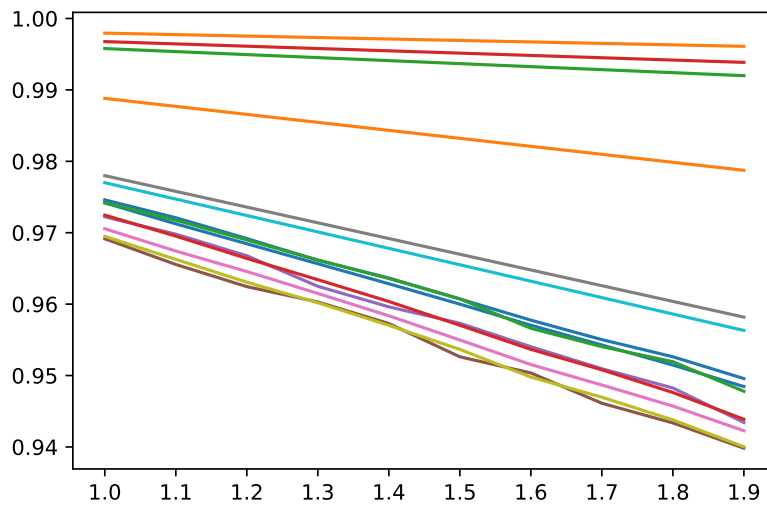


Figure 17: Asset prices in equilibrium (y-axis) for different sensitivities of prices to transacted volumes (x-axis) measured as a multiplier of the initial estimates of sensitivities (b) under a 50% outflow of wholesale funding and term corporate deposits. Each line represents an asset.

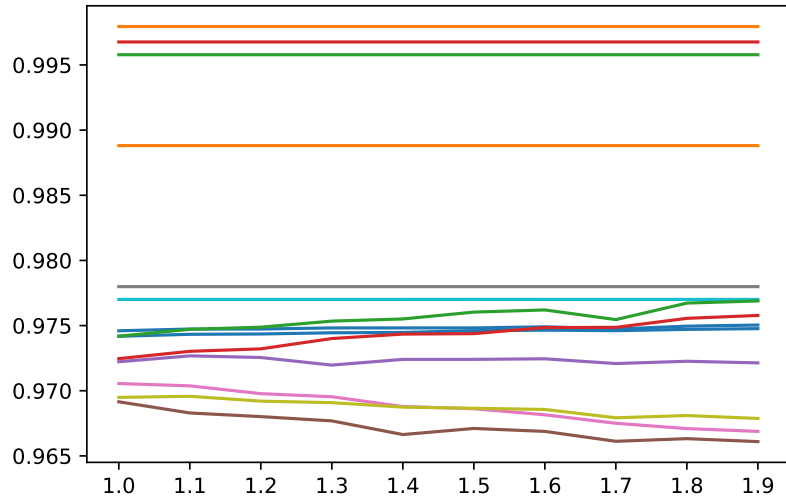


Figure 18: Asset prices in equilibrium (y-axis) for different risk aversion parameters (x-axis) measured as a multiplier of the initial calibrated values of risk aversion (γ) under a 50% outflow of wholesale funding and term corporate deposits. Each line represents an asset.

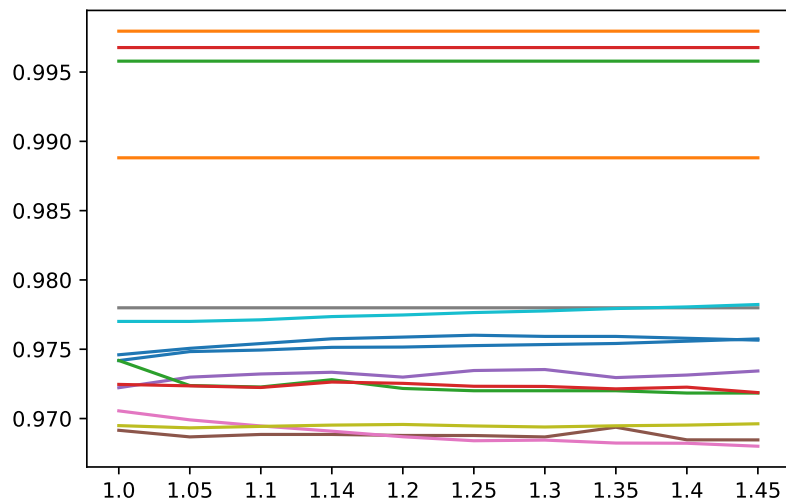
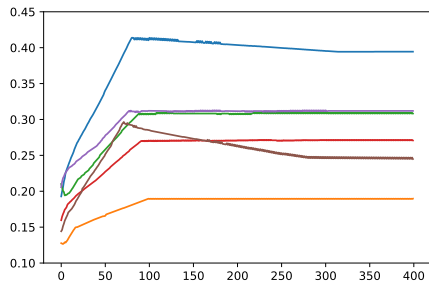
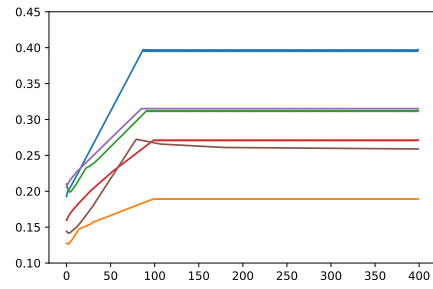


Figure 19: Asset prices in equilibrium (y-axis) for different rebound factors (x-axis) measured as a multiplier of the initial calibrated values of rebound factors (β) under a 50% outflow of wholesale funding and term corporate deposits. Each line represents an asset.



(a) With strategic interactions



(b) Without interactions

Figure 20: Cash holdings (y-axis, showing a fraction of banks' total liquid and less liquid assets, i.e., excluding loans' illiquid assets NL) in the (discretized) tâtonnement process over steps in this process (x-axis) for 25% funding shock to all banks' unsecured wholesale and corporate funding. Each line represents a bank.